# OPTIMISING FRP REINFORCEMENT LAYOUT BY USING EMBROIDERY TECHNOLOGY

Philipp Preinstorfer
TU Wien, Structural Concrete Research Group
Karlsplatz 13, E212-2
1040 Vienna, Austria
philipp.preinstorfer@tuwien.ac.at

Caroline Durnwalder - Structural Concrete Research Group, TU Wien, Vienna, Austria
Wolfgang Fiel - Polymer and Composite Research Group, University of Vienna, Vienna, Austria

**Abstract**

Fibre-reinforced polymers (FRPs) are characterised by an anisotropic behaviour, with high tensile strength in the longitudinal direction but being very sensitive to transverse pressure. Traditional reinforcement principles for steel-reinforced structures that aim at an ease of handling rather than to align the reinforcement according to the principal stresses thus result in a low utilisation rate if transferred one by one to FRP-reinforced structures. New manufacturing methods for FRP textile reinforcements, however, allow to overcome these shortcomings. In this paper, we explore the potential of embroidery technology to produce a stress-aligned FRP textile reinforcement for a simply supported beam loaded by a single load in midspan (three-point bending test). The beam itself is shape-optimised to minimise cement consumption, making the geometry more complex and thus challenging to reinforce. The optimum reinforcement design was found by linear elastic analysis of the beam and automatically manufactured according to the CAD file derived from the principal stresses. While only two-dimensional reinforcement can usually be produced with embroidery technology, a three-dimensional reinforcement cage can be created by folding the reinforcement prior to the impregnation process. The following tests on beams reinforced with such stress-aligned textiles showed very promising results. Compared to a conventional orthogonal reinforcement pattern, the failure load was more than twofold because the crack opening of the governing shear crack, which led to failure in the reference beam, could be limited with the stress-aligned reinforcement.

***Keywords:*** *textile reinforcement; textile-reinforced concrete; Embroidery; tailored fibre placement; stress-aligned reinforcement*

## 1. INTRODUCTION

In shear-critical concrete beams, stirrups are typically installed to enhance shear performance. While the direction of principal stresses is in most parts of such beams inclined to the longitudinal axis, and thus the arrangement of the stirrups in the direction of principal tensile stress would allow for good material utilisation [1], usually the stirrups are arranged in a 90° angle to ease handling. As a consequence, shear cracks that develop are inclined to the stirrup axis [2], thus inducing skew action. While this is not a major problem for steel stirrups considering the isotropic behaviour of steel, a non-alignment of anisotropic textile reinforcement results in a significant reduction of the yarn strength [3], [4], [5]. Researchers have thus looked into ways to orientate such reinforcement according to the principal stresses [6]. A promising solution can be found in the embroidery technology, where the yarn can be placed during manufacturing at random angles and orientations [7]. It is noteworthy that when optimising the reinforcement layout for a defined load case, the orientation of the reinforcement might differ substantially from the principal stresses derived from other load cases. For that reason, a base mesh is needed that sufficiently takes the stresses from other load cases while the optimised reinforcement layout is, for example, derived for the decisive load case in the ultimate limit state. In this paper we combine both reinforcement layers needed by embroidering yarns onto a base mesh. This resembles a unique approach, which has not been done before. To test the effectiveness of the measures three beams are cast and tested in the laboratory at TU Wien. While the results presented here are part of a first feasibility study, the outcome already indicates a huge potential for this technology to enhance the material utilisation of textiles in shear-critical beams.

## 2. MATERIALS AND METHODS

### 2.1. Conceptual Design

A basalt-reinforced beam with an optimized shape and reinforcement layout was developed for concentrated load applied in midspan. The tender documents of a previously conducted design competition at the RWTH Aachen University were used to define the boundary conditions [8]. Accordingly, the maximum component dimensions may not exceed 10 × 20 × 120cm³, whereby the free span was set at 1m. As a limitation, only non-metallic reinforcement was allowed to be used. To save weight, a chamfer was made along the direct connecting line between the load introduction and the supports, and the beam was designed as a hollow box girder. The thickness of the webs was chosen to be as thin as possible without impairing production, which, based on experience, resulted in a web thickness of 20mm. Figure 1 shows the geometry and reinforcement layout. Flexural capacity is enhanced by placing two basalt bars Ø16mm at the bottom chord. The reinforcement layout for the walls was derived from a linear elastic analysis of the stress distribution under the given load situation and was subsequently manufactured by the company Fiber Elements GmbH using embroidery technology. Here, the yarns that are orientated according to the main stresses are embroidered onto a planar geogrid that serves as the stitching ground (Fig. 1b). Thereafter, the textile is taken, folded over a mould to gain a reinforcement cage and coated with epoxy resin by putting it into a resin bath. Fig. 1a displays the final reinforcement layout (red for tension and blue for compression in Fig. 1). The reinforcement along the main compressive stresses is not statically needed, as the concrete is able to take the compressive stresses but was arranged to obtain a stable reinforcement cage before concreting. The intended concrete cover of the textile reinforcement was 10 mm.

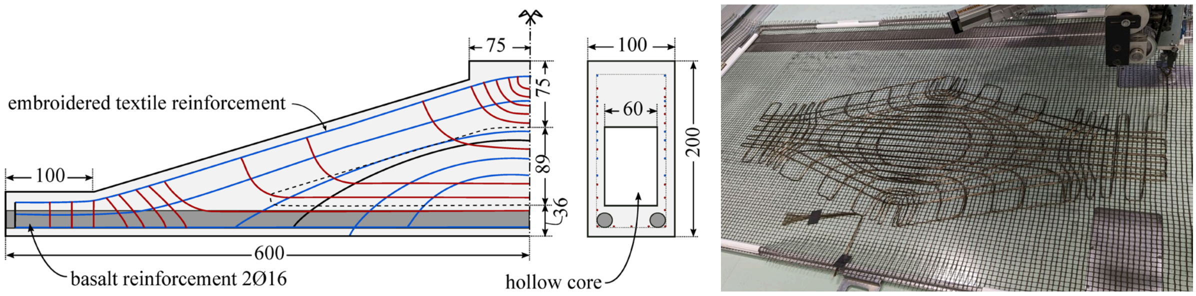


Figure 1. (a) Conceptual design of the basalt-reinforced concrete beam and (b) Fabrication of stress-aligned basalt textile reinforcement by embroidery technology (Figure taken with permission of Fiber Elements GmbH © 2023)

### 2.2. Materials

#### *2.2.1. Concrete*

A high-strength mortar type Sika Grout 312 was used with a maximum grain size of 3 mm. For casting, 25 kg of the premix was mixed with 2l of water as suggested by the manufacturer. The mortar had self-compacting properties in the fresh state, allowing to fill all the interstices of the rather complex geometry. To test the mechanical properties prisms with dimensions of 40 × 40 × 160 mm³ were cast and stored under the same conditions as the beam until time of testing. The tested flexural tensile $f_{ct,fl}$ and compressive strength $f_{cm,cube}$ is listed in Table 1. The Youngs modulus $E_{c,m}$ is taken from the manufacturers data sheet.

Table 1: Material properties of Sika Grout 312

| $f_{ct,fl}$ [MPa] | $f_{cm,cube}$ [MPa] | $E_{c,m}$ [MPa] |
|---|---|---|
| 9.65 MPa[1] | 77.47[1] | 56.000 MPa[2] |

[1]mean value of 3 samples per each of the three specimens, [2]according to data sheet of manufacturer

#### *2.2.2. Reinforcement*

Two basalt bars Ø16mm were arranged at the bottom of the beam as main tensile reinforcement. All other reinforcement types were made of 3200 tex yarns. The cross-sectional area $A_T$, tensile strength

$f_{t,u}$ and Young's modulus $E_{t,m}$ of all reinforcements is listed in Table 2. The basalt yarns that were embroidered onto the base mesh (knitted basalt geogrid) (Var. 1 - 0/90°; Var. 2 - 45° rotated) were tested under uniaxial tension. The properties of the Geogrid and the bar reinforcement were taken from the manufacturer.

Table 2: Geometric and mechanical properties of reinforcement

| Typ | $A_T$ [mm²] | $f_{t,u}$ [MPa] | $E_{t,m}$ [MPa] |
|---|---|---|---|
| Textile yarns[1] | 1,83 | 2540 | 64.000 |
| Geogrid[2] | 1,83 | 1790 | 115.000 |
| Bar reinforcement[2] | 200,96 | 1000 | 48.000 |

*[1]mean value of 3 samples, [2]according to data sheet of manufacturer*

### 2.3. Test setup

The test setup and monitoring concept can be seen in Fig. 2. The beams were supported on rollers to obtain a single-span beam with an effective length of 1m and then loaded with a single load in midspan. Three beams were produced in total. In addition to two beams with the embroidered basalt textile reinforcement, where the base mash was once rotated by 45°, a reference beam was cast where only the geogrid served as reinforcement in the wall elements. The tests were carried out in the laboratories of TU Wien, using a hydraulic testing machine. The force was applied displacement-controlled with a velocity of v = 0.5 mm/min. During testing the displacement at midspan and at the supports were recorded (Fig. 2a) using linear variable differential transformers (LVDTs). In addition, a stochastic pattern was painted on one side of the beam and photos were taken at a frequency of 5 Hz to assess the cracking process using digital image correlation (DIC) (Fig. 2b).

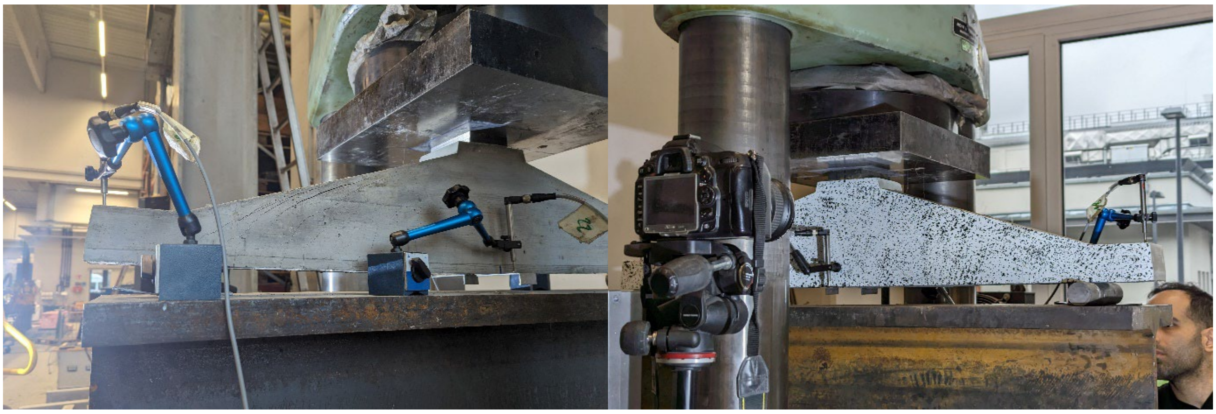

(a) (b)

Figure 2. Test setup and monitoring concept: (a) LVDTs at support and midspan and (b) stochastic pattern for DIC observation

## 3. RESULTS

### 3.1. Load-deflection behaviour

Figure 3 compares the load-deflection behaviour of all three beams tests in this series. Additionally, the results from the design contest were provided by RWTH Aachen and are displayed for comparison. A significant increase in both the bearing capacity and the stiffness can be seen. When comparing the individual variants of the optimized beam, an increase of 61% (c; trajectory + geogrid 0/90°) and 80% (b, trajectory + geogrid 45°) is obtained compared to the reference variant (a; geogrid only). Accordingly, the additional stress-aligned yarns that are embroidered onto the base mesh resulted in a significant increase in ultimate load, while the rotation of the geogrid by 45° (approximation to principal stresses) had a minor influence.

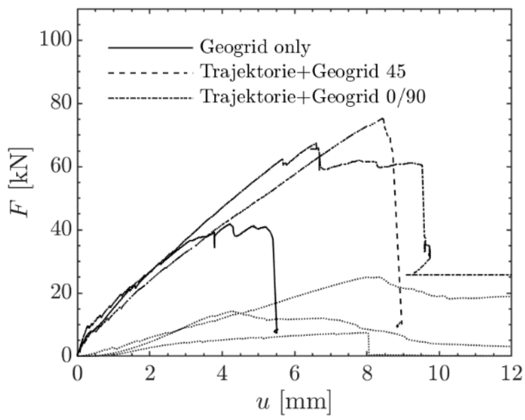


| | Type | Load F [kN] | Deflection u at $F/2$ [mm] |
|---|---|---|---|
| (a) | Geogrid | 41,85 | 1,41 |
| (b) | Trajectory+Geogrid 45 | 75,25 | 3,50 |
| (c) | Trajectory+Geogrid 0/90 | 67,61 | 2,70 |
| (d) | Design Comp. 1 | 14,23 | 2,56 |
| (e) | Design Comp. 2 | 7,43 | 2,59 |
| (f) | Design Comp. 3 | 25,02 | 4,14 |

Figure 3: Comparison of the load-deformation relationship of the basalt-reinforced beams with the beams from the design competition.

### 3.2. Failure analysis

An analysis of the cracking pattern shortly before failure confirms the effectiveness of the stress-aligned reinforcement. While in variant (a) a critical shear crack in the direction of the support led to early failure (Fig. 4a), this crack was effectively suppressed in variants (b) and (c) (Fig. 4b). The beams ultimately failed due to failure of the thin concrete compression strut, which was weakened by splitting of the concrete cover.

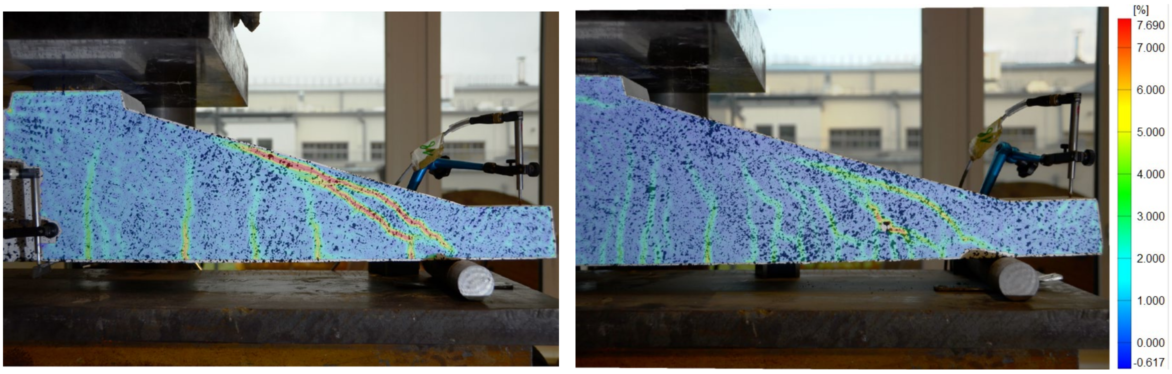


(a) (b)

Figure 4: Crack pattern before failure: (a) without and (b) with additional stress-aligned reinforcement

### 3.3. Performance assessment

Finally, the individual beams are compared with a performance indicator TP according to Eq (1), which also served as evaluation criterion in the design competition, to identify the best-performing beam:

$$TP = \frac{F_u^2}{w \cdot m} \tag{1}$$

where $F_u$ is the ultimate load, $w$ is the deflection when $F_u/2$ is reached, and $m$ is the mass of the beam. Table 3 lists the results for each beam. The mass of the beams only differed by a maximum of 30% across all variants (min. 17.78 kg vs. max. 23.55 kg).

Table 3: Performance of the beams

| | Geogrid | Traject. 45 | Traject. 0/90 | Comp.1 | Comp.2 | Comp.3 |
|---|---|---|---|---|---|---|
| mass *m* [kg] | 23,55[1] | 23,55[1] | 23,55[1] | 17,78 | 21,57 | 18,53 |
| *TP* [-] | 52.76 | 68.76 | 71.69 | 1,20 | 3,76 | 8,18 |

[1] mass *m* calculated assuming $\rho_c$ = 21 kN/m³

The comparison using the performance indicator reveals a significantly higher performance of the optimized beams examined at TU Wien, which is higher by a factor of 8.76 (71.69 for Trajekt 0/90 vs. 8.18 for Competition 3) even compared to the best performance in the competition.

## 4. CONCLUSIONS

Textile reinforcement made of high-performance fibres offer great strength and durability. The reinforcement is, however, often not utilised efficiently due to restraints in the reinforcement orientation. Embroidery technology offers the possibility to align the yarns according to the principal stresses. In this paper optimised beams utilising such reinforcement were tested and compared to the results from a design competition. Following conclusions can be drawn from these investigations:

- The beams with optimised reinforcement layout exhibited an increased ultimate load of 61% compared to a reference beam, while simultaneously only little extra reinforcement was used.
- Embroidery technology not only allows for stress-alignment of the reinforcement but also to increase reinforcement density in critically stressed areas such as areas of load introduction or support.
- While the stress-aligned reinforcement is only optimised for one particular load case, a base mesh can be used that is strong enough to carry the load from other load cases. Following this procedure, the stress-aligned reinforcement here was embroidered onto a geogrid.
- Using a performance indicator that considers the ultimate load, weight and deflection, a ~35% higher performance was obtained for the beams with the stress-aligned reinforcement compared to the beam reinforced with geogrid only.

The results demonstrate the huge potential of the embroidery technology to increase performance of structures with little extra material. This enables to create more sustainable structures. Future work must focus on an ease of the fabrication process, as a lot of manual effort was still required in this study to derive the optimum reinforcement layout and manufacture the beam.

## ACKNOWLEDGEMENTS

The authors acknowledge Rafael Ludescher for his help in casting and testing the specimens.

## DATA AVAILABILITY

The data supporting the findings of this study are available on request from the corresponding authors.

## REFERENCES

[1] S. Polónyi, ‘Zuviel Stahl im Beton?: Stahlbeton – 120 Jahre Welterfolg auf der Basis eines falschen Ansatzes’, *Beton und Stahlbetonbau*, vol. 109, no. 9, pp. 628–636, Sep. 2014, doi: 10.1002/best.201400048.

[2] P. Huber, T. Huber, and J. Kollegger, ‘Investigation of the shear behavior of RC beams on the basis of measured crack kinematics’, *Engineering Structures*, vol. 113, pp. 41–58, Apr. 2016, doi: 10.1016/j.engstruct.2016.01.025.

[3] P. Preinstorfer, P. Huber, T. Huber, B. Kromoser, and J. Kollegger, ‘Experimental investigation and analytical modelling of shear strength of thin walled textile-reinforced UHPC beams’, *Engineering Structures*, vol. 231, p. 111735, Mar. 2021, doi: 10.1016/j.engstruct.2020.111735.

[4] J. Bielak, M. Schmidt, J. Hegger, and F. Jesse, ‘Structural Behavior of Large-Scale I-Beams with Combined Textile and CFRP Reinforcement’, *Applied Sciences*, vol. 10, no. 13, p. 4625, Jul. 2020, doi: 10.3390/app10134625.

[5] C. Burgoyne, ‘Does FRP have an economic future?’, in *ACMBS MCAPC IV*, Calgary, Alberta, 2004. Accessed: Jul. 31, 2021. [Online]. Available: https://www.semanticscholar.org/paper/ACMBS-MCAPC-IV-DOES-FRP-HAVE-AN-ECONOMIC-FUTURE-Burgoyne/c6a46c418dcf6029505b6d775221354a0b6335ce

[6] L. Nahum, S. Isaac, A. Peled, and O. Amir, ‘Significant Material and Global Warming Potential Savings through Truss-Based Topology Optimization of Textile-Reinforced Concrete Beams’, *J. Compos. Constr.*, vol. 27, no. 4, p. 04023028, Aug. 2023, doi: 10.1061/JCCOF2.CCENG-4073.

[7] J. Konzilia *et al.*, ‘Embroidered Carbon Reinforcement for Concrete’, *Buildings*, vol. 13, no. 9, p. 2293, Sep. 2023, doi: 10.3390/buildings13092293.

[8] RWTH Aachen, ‘Konstruktionswettbewerb SFB TRR280’. [Online]. Available: https://www.sfbtrr280.de/fileadmin/Wettbewerb/Konstruktionswettbewerb/Konstruktionswettbewerb_2023_final_04.pdf